Biomolecules and Biomedicine
ISSN: 2831-0896 (Print) | ISSN: 2831-090X (Online)
Journal Impact Factor® (2025): 2.8
CiteScore® (2025): 4.7
www.biomolbiomed.com | blog.bjbms.org

The BiomolBiomed publishes an "Advanced Online" manuscript format as a free service to authors in order to expedite the dissemination of scientific findings to the research community as soon as possible after acceptance following peer review and corresponding modification (where appropriate). An "Advanced Online" manuscript is published online prior to copyediting, formatting for publication and author proofreading, but is nonetheless fully citable through its Digital Object Identifier (doi®). Nevertheless, this "Advanced Online" version is NOT the final version of the manuscript. When the final version of this paper is published within a definitive issue of the journal with copyediting, full pagination, etc., the new final version will be accessible through the same doi and this "Advanced Online" version of the paper will disappear.

RESEARCH ARTICLE

Zheng et al.: circFUT8 in gastric cancer

Serum circFUT8 in gastric cancer: Diagnostic performance and clinicopathological associations

Ming Zheng[1,2#], Mei Tao[3#], Shiyi Qin[1,2,4#], Xinyue Qin[1,2,4], Weiwei Zhang[1], Ruoyu Yuan[1], Shaoqing Ju[1*]

[1]Department of Laboratory Medicine, Affiliated Hospital of Nantong University, Nantong, China;

[2]Research Center of Clinical Medicine, Affiliated Hospital of Nantong University, Nantong, China;

[3]Department of Laboratory Medicine, First People's Hospital of Kunshan, Suzhou, China;

[4]Medical School, Nantong University, Nantong, China.

*Correspondence to **Shaoqing Ju**: jsq814@hotmail.com.

[#]Equally contributed to this work and share first authorship: Ming Zheng, Mei Tao, and Shiyi Qin.

DOI: https://doi.org/10.17305/bb.2026.14950

EARLY ACCESS

ABSTRACT

Gastric cancer (GC) remains a major cause of cancer-related morbidity and mortality, and biomarkers that complement current diagnostic approaches are needed. Circular RNAs (circRNAs) are promising biomarker candidates because of their stability. We characterized circFUT8 and evaluated its potential as an auxiliary serum biomarker for GC. Its circular structure and stability were assessed by back-splice junction validation, freeze-thaw and room-temperature stability assays, actinomycin D treatment, and ribonuclease R (RNase R) digestion. Real-time quantitative PCR (RT-qPCR) was used to measure circFUT8 expression in 45 pairs of GC and adjacent non-tumor tissues and in serum from 102 patients with GC, 32 patients with gastritis, and 78 healthy controls. CircFUT8 was generated by back-splicing of exons 3–6 of FUT8 and showed a distinct back-splice junction, stability under the tested conditions, and resistance to RNase R digestion. CircFUT8 expression was increased in GC tissues and serum. Serum circFUT8 distinguished GC from healthy controls, gastritis, and pooled non-GC controls, with areas under the receiver operating characteristic curve (AUCs) of 0.725, 0.756, and 0.734, respectively. Combining circFUT8 with carcinoembryonic antigen (CEA) and CA19-9 yielded the highest apparent AUC of 0.765 against healthy controls (optimism-corrected AUC, 0.756). However, the combined models did not significantly outperform circFUT8 alone. Higher serum circFUT8 levels, analyzed as a continuous variable, were associated with poorly differentiated or undifferentiated histology, lymph node metastasis, higher T stages, and advanced tumor-node-metastasis (TNM) stages. CircFUT8 also showed modest discriminatory performance for T1 and TNM stage I–II disease in exploratory analyses. These findings support serum circFUT8 as a candidate auxiliary biomarker for GC, pending validation in larger, independent cohorts.

Keywords: Gastric cancer, circFUT8, circular RNA, serum biomarker, diagnosis.

EARLY ACCESS

INTRODUCTION

Gastric cancer (GC) is one of the most common malignancies worldwide. It is estimated that approximately one million new GC cases are diagnosed annually, making it the fifth most commonly diagnosed cancer and the fifth leading cause of cancer-related deaths globally [1, 2]. Clinically, GC diagnosis relies on histological examination. However, tissue acquisition is invasive and not preferred for screening. Common approaches such as exfoliative cytology, imaging, and endoscopy are limited in sensitivity. Compounded by the absence of obvious symptoms in early-stage GC patients, many patients are often diagnosed at advanced stages. Therefore, identifying novel biomarkers to enhance the sensitivity of early GC detection is of critical importance [3-5].

Circular RNAs (circRNAs) are covalently closed RNA molecules generated from precursor mRNA through back-splicing, first identified in eukaryotic cells in 1979 [6]. With advancements in high-throughput sequencing and bioinformatics, circRNAs have increasingly been recognized as critical regulators of diverse biological processes [7-9]. Compared to linear RNAs, circRNAs lack 5' and 3' ends, rendering them more resistant to exonuclease-mediated degradation and endowing them with greater stability [10]. These characteristics have led to growing interest in circRNAs as potential disease biomarkers [11-13]. CircRNAs are also involved in a wide range of physiological and pathological processes and may function as oncogenic or tumor-suppressive regulators during tumor development and progression [14-17]. In addition, circRNAs often exhibit tissue-specific or organ-specific expression patterns, and the same circRNA may exert distinct biological effects in different tumor types. These properties highlight their potential as diagnostic biomarkers and therapeutic targets in GC [18-21].

A previous circRNA microarray analysis of three pairs of poorly differentiated gastric adenocarcinoma and matched adjacent non-tumor tissues showed that hsa_circ_0102434 was significantly upregulated in tumor tissues [22]. Database and sequence analyses indicated that hsa_circ_0102434 (circFUT8) is generated by back-splicing of exons 3-6 of the fucosyltransferase 8 (FUT8) gene. FUT8 is the key enzyme responsible for core fucosylation, and its dysregulation has been implicated in the development and progression of multiple malignancies [23, 24]. However, the

EARLY ACCESS

circular structure and stability of circFUT8, as well as its potential utility as an auxiliary diagnostic biomarker for GC, have not been systematically investigated.

In this study, we validated the circular structure of circFUT8 and assessed its stability under experimental and preanalytical conditions. We then measured circFUT8 expression in GC tissues and patient serum, evaluated its diagnostic performance alone and in combination with CEA and CA19-9, and investigated associations with clinicopathological characteristics. We also explored the ability of circFUT8 to identify T1-stage and TNM stage I-II GC, with the aim of supporting its further evaluation as a novel serum biomarker for the auxiliary diagnosis of GC.

MATERIALS AND METHODS

Study population and eligibility criteria

All specimens for this study were obtained from patients and healthy examinees who visited the Affiliated Hospital of Nantong University between 2018 and 2022. This study collected 45 paired GC tissue specimens and 212 serum samples, comprising 102 from GC patients, 78 from healthy controls, and 32 from patients with gastritis. The tissue and GC serum cohorts comprised different participants, with no overlap between them. Patients with GC were included if they had newly diagnosed primary GC confirmed by histopathological examination of endoscopic biopsy or surgical specimens and had complete clinicopathological data. Gastritis was confirmed by endoscopy and histopathological examination, and patients with malignancy or high-grade intraepithelial neoplasia were excluded from the gastritis group. Healthy controls were individuals undergoing routine health examinations during the same period with no history of malignancy, no gastrointestinal symptoms, and normal results on complete blood count and liver and renal function tests. Exclusion criteria included a history of malignancy other than GC, acute infection, systemic autoimmune or inflammatory disease, severe cardiac, hepatic, or renal dysfunction, and pregnancy.

Serum sample processing and storage

Blood samples from GC patients were collected before surgery, chemotherapy, radiotherapy, or any other anticancer treatment. Whole blood samples were allowed to clot for 30 min and centrifuged at 3,000 × *g* for 10 min at 4°C to obtain serum.

EARLY ACCESS

Hemolysis in serum samples was assessed using an AU5800 chemistry analyzer (Beckman Coulter). Samples with a hemolysis (HEM) grade of + or higher were excluded. Serum samples were transferred to RNase-free tubes and stored at -80 °C until RNA extraction. Samples were thawed on ice before extraction, and repeated freeze-thaw cycles were avoided.

Measurement of serum CEA and CA19-9

Serum carcinoembryonic antigen (CEA) and carbohydrate antigen 19-9 (CA19-9) concentrations were measured using chemiluminescent microparticle immunoassay (CMIA) on an ARCHITECT i2000 analyzer (Abbott Laboratories, USA). The positivity cutoffs for the threshold-based diagnostic analyses were 5 ng/mL for CEA and 37 U/mL for CA19-9.

Cell lines

MKN-45 and AGS cells were obtained from the Stem Cell Bank of the Chinese Academy of Sciences (Shanghai, China), authenticated by STR profiling and tested negative for mycoplasma.

Total RNA extraction

Each 300 µL serum sample was mixed with 1 mL TRIzol LS Reagent (Invitrogen, Canada) and lysed on ice for 5 min. Chloroform (200 µL) was added. Samples were vortexed for 15 s, incubated on ice for 2-3 min, and centrifuged at 12,000 rpm for 15 min at 4 °C. The aqueous phase (500 µL) was mixed with 500 µL isopropanol, incubated on ice for 15 min, and centrifuged at 12,000 rpm for 10 min at 4 °C. Pellets were washed with 1 mL 75% ethanol, centrifuged at 7,500 rpm for 10 min at 4 °C, dried at 50 °C for 5-10 min, and dissolved in 15 µL diethyl pyrocarbonate-treated water at 60 °C for 5-10 min. RNA concentration and purity were determined using a NanoDrop 2000 spectrophotometer (Thermo Fisher Scientific).

Reverse transcription

Reverse transcription was performed with a Thermo Fisher Scientific kit (MA, USA), typically using 1,000 ng RNA, at 25 °C for 5 min, 42 °C for 60 min, and 70 °C for 5 min, and maintenance at 4 °C.

EARLY ACCESS

Real-time quantitative PCR (RT-qPCR)

Each 20 μL amplification mixture contained 10 μL ChamQ Universal SYBR qPCR Master Mix, 0.5 μL each of 10 μM forward and reverse primers, 4 μL DEPC-treated water, and 5 μL cDNA. Amplification was performed with an initial denaturation at 95°C for 5 min, followed by 45 cycles of 95°C for 15 s and 58°C for 34 s. Melting-curve analysis was performed after amplification. 18S rRNA was used as the reference gene. Relative circFUT8 expression was calculated using the $2^{-\Delta\Delta Ct}$ method, where ΔCt was calculated as $Ct_{\text{circFUT8}} - Ct_{\text{18S rRNA}}$, and $\Delta\Delta Ct$ was calculated as $\Delta Ct_{\text{sample}}$ − mean $\Delta Ct_{\text{control group}}$. For serum and tissue analyses, the control-group mean ΔCt was calculated from healthy controls and adjacent non-tumor tissues, respectively. Amplification efficiencies, determined from standard curves generated using a five-point, four-fold serial dilution series, were 94.7% for circFUT8 and 96.3% for 18S rRNA, with $R^2 > 0.99$ for both assays. Each sample was analyzed in technical triplicate, and the mean *Ct* values were used for subsequent calculations. Primer sequences are listed as follows: circFUT8-F: CAGACAGATGGAGCAGGTGAT, circFUT8-R: CATGCGCTCTACATGCTGAA, FUT8-F: GTTCAAGTGGTCGAGCTTCC, FUT8-R: GCGAGGTCTTCTGGTACAGC, 18S rRNA-F: CGGCTACCACATCCAAGGAA, 18S rRNA-R: GCTGGAATTACCGCGGCT, GAPDH-convergent-F: CAGGAGGCATTGCTGATGAT, GAPDH-convergent-R: GAAGGCTGGGGCTCATTT, GAPDH-divergent-F: TCCTCACAGTTGCCATGTAGACCC, GAPDH-divergent-R: TGCGGGCTCAATTTATAGAAACCGGG.

Actinomycin D stability assay

Cells were treated with 2.5 μg/mL actinomycin D (Geneseed Biotech, Guangzhou, China) and RNA was collected at 0, 2, 4, 8, 12, and 24 h.

Ribonuclease R (RNase R) digestion assay

The 50 μL reaction mixture contained 10 μg RNA, 5 μL 10× Reaction Buffer, RNase R (20 U/μL; 3-4 μL per μg RNA, Thermo Fisher Scientific), and RNase-free water. Samples were incubated at 37 °C for 30 min followed by 70 °C for 10 min before reverse transcription.

EARLY ACCESS

Freeze-thaw stability assay

Homogenized serum was divided into five tubes assigned to 0, 1, 3, 5, or 10 freeze-thaw cycles. The 0-cycle aliquot was lysed immediately in 1 mL TRIzol LS and stored at -80 °C. After the assigned cycles, TRIzol LS was added and all aliquots underwent RNA extraction, reverse transcription, and RT-qPCR in parallel to minimize inter-assay variation.

Room-temperature stability assay

Homogenized serum was divided into five tubes and incubated at room temperature for 0, 6, 12, 18, or 24 h. Aliquots were lysed at the assigned times and then processed together for RNA extraction, reverse transcription, and RT-qPCR. Target cycle-threshold (Ct) values were compared among time points.

Ethical statement

This study was conducted in accordance with the Declaration of Helsinki and was approved by the Ethics Committee of the Affiliated Hospital of Nantong University (approval No. 2018-L055). The requirement for informed consent was waived by the ethics committee.

Statistical analysis

Statistical analyses were performed using GraphPad Prism 9.0 and R 4.6.0. Comparisons between two independent groups were performed using the Mann-Whitney U test, whereas paired samples were compared using the Wilcoxon matched-pairs signed rank test. Comparisons among three or more independent groups were performed using the Kruskal-Wallis test followed by Dunn's multiple-comparison test, where appropriate. Associations between categorical variables were evaluated using the chi-square test. *p* values for clinicopathological associations and DeLong AUC comparisons were adjusted using the Holm method.

ROC curve analysis was performed to evaluate diagnostic performance, and AUCs with 95% CIs were calculated. Combined models were constructed using logistic regression with biomarker levels as continuous predictors, and ROC curves were generated from the predicted probabilities of these models. Internal validation used 1,000 bootstrap resamples to estimate optimism-corrected AUCs.

EARLY ACCESS

In a separate cutoff-based analysis, sensitivity, specificity, accuracy, positive predictive value (PPV), and negative predictive value (NPV) were calculated with 95% CIs. Combinations were considered positive if any constituent marker was positive (OR rule). The prespecified clinical cutoffs were used for CEA and CA19-9, and the circFUT8 cutoff (1.0745) was selected by maximizing the Youden index for distinguishing patients with GC from healthy controls. The 95% CIs were calculated using the Clopper-Pearson method for sensitivity, specificity, and accuracy and the standard logit method for PPV and NPV.

All statistical tests were two-sided, and $p < 0.05$ was considered statistically significant.

RESULTS

Identification of circFUT8 and validation of its circular structure

A circRNA expression profiling study using three pairs of poorly differentiated gastric adenocarcinoma and matched adjacent non-tumor tissues identified that hsa_circ_0102434 (circFUT8) was significantly upregulated in tumor tissues [22]. According to circBase and circPrimer analysis, circFUT8 is located on chromosome 14 and is generated by back-splicing of exons 3-6 of the FUT8 gene, with a full length of 824 nt (Figure 1A). Divergent primers spanning the back-splice junction amplified a PCR product of the expected size (Figure 1B), and Sanger sequencing confirmed the back-splice junction (Figure 1C). PCR using cDNA and genomic DNA (gDNA) further showed that divergent primers generated the expected circFUT8 product from cDNA but not gDNA (Figure 1D). These findings support the identity of circFUT8 as a circular RNA generated by back-splicing.

Stability of circFUT8

To assess the feasibility of circFUT8 as a serum biomarker, we first evaluated its stability under different experimental conditions [10, 25, 26]. Within the tested range of freeze-thaw cycles and room-temperature incubation times, no significant changes were observed in the serum circFUT8 cycle threshold (Ct) values (Figure 2A, 2B). Following actinomycin D treatment, the reduction in circFUT8 was markedly smaller than that in FUT8 mRNA (Figure 2C), and after RNase R digestion, the relative level of circFUT8 remaining was higher than that of linear FUT8 mRNA (Figure 2D).

EARLY ACCESS

These results indicate that circFUT8 was stable under the tested preanalytical conditions and more resistant to degradation than its cognate linear transcript.

CircFUT8 is upregulated in GC tissues and patient serum

In 45 pairs of GC and paired adjacent non-tumor tissues, the relative expression of circFUT8 was significantly higher in tumor tissues (Figure 3A). Serum circFUT8 expression was also significantly higher in patients with GC than in both control groups. When healthy controls and patients with gastritis were combined into a single non-GC control group, serum circFUT8 levels remained significantly higher in patients with GC than in the pooled control group (Figure 3B, 3C). The consistent elevation of circFUT8 in GC tissues and serum supports its further evaluation as a potential serum biomarker for the auxiliary diagnosis of GC.

Diagnostic performance of serum circFUT8 for GC

ROC curve analysis showed that serum circFUT8 distinguished patients with GC from healthy controls, patients with gastritis, and the combined non-GC control group, with AUCs of 0.725 (95% confidence interval [CI], 0.651-0.800), 0.756 (95% CI, 0.647-0.864), and 0.734 (95% CI, 0.668-0.800), respectively (Figure 4A). As shown in Figure 4B, when healthy donors were used as the control group, the AUC for circFUT8 was 0.725 (95% CI, 0.651-0.800), which was higher than the AUCs for CEA and CA19-9 alone (0.685 [95% CI, 0.608-0.762] and 0.606 [95% CI, 0.524-0.689], respectively).

The logistic regression model combining circFUT8 with CEA yielded an apparent AUC of 0.746 (95% CI, 0.676-0.817), and the combination of circFUT8 with CA19-9 yielded an AUC of 0.731 (95% CI, 0.658-0.803), both of which were higher than those of the corresponding conventional markers alone. The combination of circFUT8, CEA, and CA19-9 yielded the highest AUC of 0.765 (95% CI, 0.697-0.833; Figure 4C, 4D). After internal validation, the corresponding optimism-corrected AUCs were 0.743 (95% CI, 0.664-0.818), 0.728 (95% CI, 0.654-0.803), and 0.756 (95% CI, 0.687-0.832), respectively (Table 1). Paired DeLong tests with Holm correction showed that the combination of circFUT8 with CA19-9 outperformed CA19-9 alone (adjusted $p = 0.004$). Neither the combination of circFUT8 with CEA versus CEA alone nor the three-marker model versus the combination of CEA with CA19-9

EARLY ACCESS

showed a statistically significant difference (both adjusted $p = 0.061$). None of the three models incorporating circFUT8 differed significantly from circFUT8 alone.

In the separate cutoff-based analysis (Table 2), combining circFUT8 with CEA using the OR rule increased sensitivity from 66.67% to 92.16%, and combining circFUT8 with CA19-9 increased sensitivity from 23.53% to 78.43%. These increases in sensitivity were accompanied by lower specificity. The three-marker combination yielded a sensitivity of 92.16%, with no further increase in sensitivity over the combination of circFUT8 with CEA.

Association between serum circFUT8 expression and clinicopathological characteristics

To assess the associations between serum circFUT8 levels and clinicopathological characteristics, serum circFUT8 was first treated as a continuous variable, and its relative levels were compared across clinicopathological subgroups. After Holm correction, serum circFUT8 levels were significantly higher in patients with poorly differentiated or undifferentiated tumors, lymph node metastasis, higher T stage, or TNM stage III-IV disease (Figure 5). Serum circFUT8 levels were also higher in patients with perineural and/or vascular invasion in the unadjusted analysis, although this difference was not statistically significant after Holm correction (Table S1). No significant difference in serum circFUT8 levels was observed according to tumor size.

In an exploratory analysis, the 102 patients with GC were divided into high-expression and low-expression groups using the median serum circFUT8 level as the cutoff. Chi-square tests with Holm correction showed that only tumor differentiation remained significantly associated with circFUT8 expression, whereas the associations with lymph node metastasis and TNM stage did not reach statistical significance after correction (Table 3). These findings, based primarily on the analysis of circFUT8 as a continuous variable, indicate that elevated serum circFUT8 levels are associated with adverse clinicopathological features of GC. Serum circFUT8 may therefore reflect, at least in part, tumor aggressiveness and more advanced GC.

Auxiliary diagnostic value of serum circFUT8 for T1 and TNM stage I–II GC

To evaluate the potential auxiliary diagnostic value of serum circFUT8 in early GC, we performed exploratory subgroup analyses using depth of tumor invasion and

EARLY ACCESS

overall TNM stage as two complementary criteria. We then separately assessed serum circFUT8 levels in patients with T1 GC and those with TNM stage I–II GC and evaluated its diagnostic performance in each subgroup. Serum circFUT8 levels were higher in patients with T1 GC than in healthy controls and patients with gastritis (Figure 6A). ROC curve analysis yielded AUCs ranging from 0.662 to 0.708 for distinguishing patients with T1 GC from the three control groups, suggesting modest discriminatory performance in this subgroup (Figure 6B). Similar results were obtained for patients with TNM stage I–II GC, who exhibited elevated serum circFUT8 levels relative to the control groups, with ROC curve analysis demonstrating comparable discriminatory performance (Figure 6C, 6D). AUC estimates with 95% CIs are reported in Table S2. These results suggest that serum circFUT8 may have auxiliary diagnostic value for T1 GC and earlier TNM-stage GC. However, given the small subgroup sizes, these findings warrant further validation in larger, independent cohorts.

DISCUSSION

GC remains a major cause of cancer-related morbidity and mortality worldwide [1]. Due to the atypical early symptoms of GC and the low sensitivity of conventional screening methods such as tumor marker detection, imaging examinations, and endoscopy, GC patients are often diagnosed at an advanced stage and consequently have a poor prognosis [4, 5, 27]. Biomarkers that can assist in the early diagnosis of GC are therefore urgently needed. CircRNAs have attracted considerable attention as potential biomarkers in multiple cancers [28, 29]. Their relatively long half-lives and resistance to degradation make them attractive candidates for clinical application [8, 9]. In the present study, we characterized circFUT8 (hsa_circ_0102434) and evaluated its potential as an adjunctive diagnostic biomarker for GC.

CircFUT8 is an 824-nt transcript generated by back-splicing of exons 3-6 of FUT8. Amplification with divergent primers, AGE, Sanger sequencing, and gDNA assays collectively confirmed its circular RNA features and provided the foundation for subsequent analyses of expression and clinical value [25, 26, 30].

The suitability of a serum biomarker depends partly on its stability during sample collection, storage, and processing. Serum circFUT8 Ct values did not change significantly across the tested freeze-thaw cycles or room-temperature incubation

EARLY ACCESS

periods, suggesting that serum circFUT8 is relatively robust under these common preanalytical conditions. Following actinomycin D treatment, circFUT8 levels declined more slowly than linear FUT8 mRNA levels. After RNase R digestion, the proportion of circFUT8 remaining was also greater than that of linear FUT8 mRNA. These findings are consistent with the characteristically slower degradation and greater resistance to RNase R digestion of circRNAs and further support the molecular stability of circFUT8.

CircFUT8 expression was significantly higher in GC tissues than in paired adjacent non-tumor tissues. Serum circFUT8 levels were also significantly higher in patients with GC than in healthy controls and patients with benign gastric disease, and the difference remained significant when the two control groups were combined. The consistent elevation of circFUT8 in GC tissues and serum supports an association between circFUT8 upregulation and GC and indicates that elevated circFUT8 levels are detectable in circulation.

Serum circFUT8 yielded AUCs of 0.725, 0.756, and 0.734 for distinguishing patients with GC from healthy controls, patients with gastritis, and the pooled non-GC control group, respectively. When healthy controls were used as the reference group, circFUT8 yielded a higher AUC than either CEA or CA19-9. Logistic regression models combining circFUT8 with either marker increased the AUC relative to the corresponding single-marker test. The three-marker panel achieved the highest AUC of 0.765, with an optimism-corrected AUC of 0.756. However, only the AUC comparison between the combination of circFUT8 with CA19-9 and CA19-9 alone remained statistically significant after Holm correction. These results suggest that circFUT8 may provide complementary diagnostic information, particularly alongside CA19-9. None of the combined models significantly outperformed circFUT8 alone, and the relatively small AUC gains suggest that CEA and CA19-9 may provide limited additional discriminatory information beyond circFUT8 in this cohort, possibly reflecting overlapping diagnostic information. The incremental value of these combinations requires external validation. In the separate cutoff-based analysis, combining the markers using the OR rule increased sensitivity at the cost of a reduction in specificity. In addition, the observed PPV and NPV reflect the case-control composition of this study and should not be directly extrapolated to clinical or screening populations.

EARLY ACCESS

Serum circFUT8 levels were also associated with several adverse clinicopathological characteristics. When analyzed as a continuous variable, serum circFUT8 levels were significantly higher in patients with poor or undifferentiated histology, lymph node metastasis, T3-T4 disease, and TNM stage III–IV disease. In the exploratory median-based dichotomization, however, only the association with tumor differentiation remained significant after Holm correction. This discrepancy may reflect the loss of information and statistical power resulting from dichotomization, together with the limited and imbalanced subgroup sizes. Overall, these findings suggest that, in addition to distinguishing GC from controls, serum circFUT8 may reflect differences in tumor differentiation and stage.

Given the importance of early detection in improving the management of GC, we further evaluated serum circFUT8 levels and diagnostic performance in patients with T1 GC and those with TNM stage I–II GC. The exploratory analyses showed that serum circFUT8 levels in both subgroups were elevated relative to controls, with AUCs ranging from 0.662 to 0.708 for T1 GC and from 0.647 to 0.702 for TNM stage I–II GC. The T1 category primarily reflects the depth of invasion of the primary tumor, whereas TNM stage I–II represents an integrated staging category that also incorporates lymph node status. Therefore, the two patient groups are not equivalent. Evaluating both groups allowed us to explore the discriminatory potential of serum circFUT8 in earlier-stage GC from complementary staging perspectives. However, given the small subgroup sizes, these findings do not establish a role for serum circFUT8 in early detection. Future studies should validate its performance in independent cohorts and determine whether combining circFUT8 with CEA, CA19-9, or other biomarkers can improve diagnostic performance in these patient populations.

Limitations

This study has several limitations. First, this was a single-center study without an independent validation cohort. Despite bootstrap internal validation, the data-derived circFUT8 cutoff and combined models require external validation. Second, *n*o formal a priori sample-size calculation was performed, and the T1, TNM stage I–II, and several clinicopathological subgroups were relatively small. These subgroup analyses, including the median-based dichotomization, should therefore be considered exploratory. Third, the case-control composition does not reflect the prevalence of GC

EARLY ACCESS

in clinical or screening populations, so the observed PPV and NPV cannot be generalized. Fourth, the primarily cross-sectional design precluded determination of whether circFUT8 upregulation contributes to GC development or progression. Longitudinal data, including changes in serum circFUT8 levels before and after treatment and long-term follow-up data, were unavailable, preventing evaluation of its potential utility for treatment monitoring and prognostic assessment. Finally, the biological function of circFUT8 in GC and its relationship with its host gene, FUT8, remain to be elucidated through cellular and animal studies.

CONCLUSION

CircFUT8 is a stable circular RNA that is upregulated in GC tissues and elevated in the serum of patients with GC. Serum circFUT8 showed potential as an auxiliary diagnostic biomarker and may provide complementary diagnostic information when combined with CEA and CA19-9. Its associations with poor differentiation, lymph node metastasis, and advanced T and TNM stages further suggest potential clinical relevance. These findings support serum circFUT8 as a candidate auxiliary biomarker for GC diagnosis, and its diagnostic performance and clinical utility require confirmation in larger, independent cohorts.

Conflicts of interest: Authors declare no conflicts of interest.

Funding: This work was supported by the National Natural Science Foundation of China (grant numbers 82472356, 82272411), Postgraduate Research and Practice Innovation Program of Jiangsu Province (grant numbers KYCX24_3582), Jiangsu Province Medical Key Discipline (Laboratory) (grant numbers ZDXK202240), Science and Technology Project of Jiangsu Province (grant numbers BE2023741), Foundation of Jiangsu Province Research Hospital (grant numbers YJXYY202204-XKB16) and Science and Technology Project of Nantong (grant numbers MSZ2024012).

Data availability: The data generated and analyzed during the current study are available from the corresponding author on reasonable request.

Artificial intelligence (AI) use statement: The authors used ChatGPT (OpenAI) to assist in drafting the response to reviewers and in language editing of the revised manuscript. The authors reviewed and edited all content and take full responsibility for the publication.

EARLY ACCESS

Submitted: August 29, 2026
Accepted: November 5, 2026
Published online: November 12, 2026

EARLY ACCESS

REFERENCES

1. Bray F, Laversanne M, Sung H, Ferlay J, Siegel RL, Soerjomataram I, et al. Global cancer statistics 2022: GLOBOCAN estimates of incidence and mortality worldwide for 36 cancers in 185 countries. CA Cancer J Clin. 2024;74(3):229–63. https://doi.org/10.3322/caac.21834

2. Siegel RL, Kratzer TB, Giaquinto AN, Sung H, Jemal A. Cancer statistics, 2025. CA Cancer J Clin. 2025;75(1):10–45. https://doi.org/10.3322/caac.21871

3. Morgan DR, Corral JE, Li D, Montgomery EA, Riquelme A, Kim JJ, et al. ACG Clinical Guideline: Diagnosis and Management of Gastric Premalignant Conditions. Am J Gastroenterol. 2025;120(4):709–37. https://doi.org/10.14309/ajg.0000000000003350

4. Lordick F, Carneiro F, Cascinu S, Fleitas T, Haustermans K, Piessen G, et al. Gastric cancer: ESMO Clinical Practice Guideline for diagnosis, treatment and follow-up. Ann Oncol. 2022;33(10):1005–20. https://doi.org/10.1016/j.annonc.2022.07.004

5. Shitara K, Fleitas T, Kawakami H, Curigliano G, Narita Y, Wang F, et al. Pan-Asian adapted ESMO Clinical Practice Guidelines for the diagnosis, treatment and follow-up of patients with gastric cancer. ESMO Open. 2024;9(2):102226. https://doi.org/10.1016/j.esmoop.2023.102226

6. Hsu MT, Coca-Prados M. Electron microscopic evidence for the circular form of RNA in the cytoplasm of eukaryotic cells. Nature. 1979;280(5720):339–40. https://doi.org/10.1038/280339a0

7. Memczak S, Jens M, Elefsinioti A, Torti F, Krueger J, Rybak A, et al. Circular RNAs are a large class of animal RNAs with regulatory potency. Nature. 2013;495(7441):333–8. https://doi.org/10.1038/nature11928

8. Conn VM, Chinnaiyan AM, Conn SJ. Circular RNA in cancer. Nat Rev Cancer. 2024;24(9):597–613. https://doi.org/10.1038/s41568-024-00721-7

9. Liu CX, Chen LL. Circular RNAs: Characterization, cellular roles, and applications. Cell. 2022;185(12):2016–34. https://doi.org/10.1016/j.cell.2022.04.021

EARLY ACCESS

10. Ren L, Jiang Q, Mo L, Tan L, Dong Q, Meng L, et al. Mechanisms of circular RNA degradation. Commun Biol. 2022;5(1):1355. https://doi.org/10.1038/s42003-022-04262-3

11. Sui S, Li Y, Maurel J, Goel A. circ-EGFR is a predictor of response to Cetuximab and a potential target in colorectal cancer. EMBO Mol Med. 2025;17(12):3525–54. https://doi.org/10.1038/s44321-025-00333-0

12. Guo P, Jia X, Wang S, Li X, Liu Y, Lin L, et al. CircSMEK1 suppresses HCC via the hnRNPK-IGF2-AKT axis: a diagnostic biomarker and therapeutic target. Adv Sci (Weinh). 2025;12(48):e05267. https://doi.org/10.1002/advs.202505267

13. Baci D, Tastsoglou S, Provenzano C, Perfetti A, Izzo M, Lisanti M, et al. circARHGAP10 as a candidate biomarker and therapeutic target in myotonic dystrophy type 1. Mol Ther Nucleic Acids. 2025;36(3):102646. https://doi.org/10.1016/j.omtn.2025.102646

14. Guo X, Xi L, Liu Y, Lv W, Li T, Ju A, et al. Dysregulation of CircZNF79(5) modulates YBX1 stability and selective autophagy to drive hepatocellular carcinoma progression. Adv Sci (Weinh). 2026;13(6):e10310. https://doi.org/10.1002/advs.202510310

15. Hansen TB, Jensen TI, Clausen BH, Bramsen JB, Finsen B, Damgaard CK, et al. Natural RNA circles function as efficient microRNA sponges. Nature. 2013;495(7441):384–8. https://doi.org/10.1038/nature11993

16. Du WW, Yang W, Liu E, Yang Z, Dhaliwal P, Yang BB. Foxo3 circular RNA retards cell cycle progression via forming ternary complexes with p21 and CDK2. Nucleic Acids Res. 2016;44(6):2846–58. https://doi.org/10.1093/nar/gkw027

17. Yang Y, Fan X, Mao M, Song X, Wu P, Zhang Y, et al. Extensive translation of circular RNAs driven by N(6)-methyladenosine. Cell Res. 2017;27(5):626–41. https://doi.org/10.1038/cr.2017.31

18. Wang Y, Zhang J, Yang Y, Liu Z, Sun S, Li R, et al. Circular RNAs in human diseases. MedComm (2020). 2024;5(9):e699. https://doi.org/10.1002/mco2.699

EARLY ACCESS

19. Kristensen LS, Jakobsen T, Hager H, Kjems J. The emerging roles of circRNAs in cancer and oncology. Nat Rev Clin Oncol. 2022;19(3):188–206. https://doi.org/10.1038/s41571-021-00585-y

20. Hanniford D, Ulloa-Morales A, Karz A, Berzoti-Coelho MG, Moubarak RS, Sánchez-Sendra B, et al. Epigenetic silencing of CDR1as drives IGF2BP3-mediated melanoma invasion and metastasis. Cancer Cell. 2020;37(1):55–70.e15. https://doi.org/10.1016/j.ccell.2019.12.007

21. Li P, Yang X, Yuan W, Yang C, Zhang X, Han J, et al. CircRNA-Cdr1as exerts anti-oncogenic functions in bladder cancer by sponging microRNA-135a. Cell Physiol Biochem. 2018;46(4):1606–16. https://doi.org/10.1159/000489208

22. Zhang C, Wang J, Geng X, Tu J, Gao H, Li L, et al. Circular RNA expression profile and m6A modification analysis in poorly differentiated adenocarcinoma of the stomach. Epigenomics. 2020;12(12):1027–40. https://doi.org/10.2217/epi-2019-0153

23. Zhao YP, Xu XY, Fang M, Wang H, You Q, Yi CH, et al. Decreased core-fucosylation contributes to malignancy in gastric cancer. PLoS One. 2014;9(4):e94536. https://doi.org/10.1371/journal.pone.0094536

24. Liao C, An J, Yi S, Tan Z, Wang H, Li H, et al. FUT8 and protein core fucosylation in tumours: from diagnosis to treatment. J Cancer. 2021;12(13):4109–20. https://doi.org/10.7150/jca.58268

25. Nielsen AF, Bindereif A, Bozzoni I, Hanan M, Hansen TB, Irimia M, et al. Best practice standards for circular RNA research. Nat Methods. 2022;19(10):1208–20. https://doi.org/10.1038/s41592-022-01487-2

26. Jeck WR, Sorrentino JA, Wang K, Slevin MK, Burd CE, Liu J, et al. Circular RNAs are abundant, conserved, and associated with ALU repeats. RNA. 2013;19(2):141–57. https://doi.org/10.1261/rna.035667.112

27. Darvishi A, Dadashzadeh Asl A, Golshaniniya P, Alipour A, Naseri A, Hamzehzadeh S, et al. Serum markers and gastric cancer: an umbrella review. BMC Gastroenterol. 2025;25(1):737. https://doi.org/10.1186/s12876-025-04349-1

EARLY ACCESS

28. Yuan S, Li L, Bai X, Gu W. BloodCircR: A comprehensive database for human peripheral blood circular RNAs. iScience. 2025;28(11):113742. https://doi.org/10.1016/j.isci.2025.113742

29. Zhang J, Luo Z, Zheng Y, Duan M, Qiu Z, Huang C. CircRNA as an Achilles heel of cancer: characterization, biomarker and therapeutic modalities. J Transl Med. 2024;22(1):752. https://doi.org/10.1186/s12967-024-05562-4

30. Chen LL, Bindereif A, Bozzoni I, Chang HY, Matera AG, Gorospe M, et al. A guide to naming eukaryotic circular RNAs. Nat Cell Biol. 2023;25(1):1–5. https://doi.org/10.1038/s41556-022-01066-9

EARLY ACCESS

TABLES AND FIGURES WITH LEGENDS

Table 1. Bootstrap internal validation and DeLong comparisons of combined logistic regression models

Model	Apparent AUC	Optimism-corrected AUC (95% CI)	DeLong *p* vs. circFUT8 (adjusted *p*)	Reference model	DeLong *p* vs. reference model (adjusted *p*)
circFUT8 + CEA	0.746	0.743 (0.664–0.818)	0.532 (1.000)	CEA	0.012 (0.061)
circFUT8 + CA19-9	0.731	0.728 (0.654–0.803)	0.852 (1.000)	CA19-9	<0.001 (0.004)
circFUT8 + CEA + CA19-9	0.765	0.756 (0.687–0.832)	0.269 (0.808)	CEA + CA19-9	0.015 (0.061)

Optimism-corrected AUCs were estimated using 1,000 stratified bootstrap resamples, with 95% CIs obtained by nested bootstrap. Apparent AUCs were compared using paired DeLong tests. *p* values are unadjusted, with Holm-adjusted *p* values for the six comparisons shown in parentheses. **Abbreviations**: AUC, area under the receiver operating characteristic curve; CA19-9, carbohydrate antigen 19-9; CEA, carcinoembryonic antigen; CI, confidence interval; circFUT8, circular RNA derived from FUT8.

EARLY ACCESS

Table 2. Diagnostic performance of serum circFUT8, CEA, and CA19-9 alone and in OR-rule combinations for distinguishing patients with GC (*n* = 102) from healthy controls (*n* = 78)

Marker or combination	SEN (%)	SPE (%)	ACCU (%)	PPV (%)	NPV (%)
circFUT8	75.49 (65.98–83.47)	60.26 (48.54–71.17)	68.89 (61.58–75.57)	71.30 (64.91–76.93)	65.28 (56.12–73.43)
CEA	66.67 (56.64–75.69)	53.85 (42.18–65.21)	61.11 (53.58–68.27)	65.38 (58.90–71.34)	55.26 (46.72–63.51)
CA19-9	23.53 (15.69–32.96)	83.33 (73.19–90.82)	49.44 (41.93–56.98)	64.86 (50.15–77.21)	45.45 (41.85–49.10)
circFUT8 + CEA	92.16 (85.13–96.55)	35.90 (25.34–47.56)	67.78 (60.42–74.54)	65.28 (61.20–69.14)	77.78 (62.82–87.88)
circFUT8 + CA19-9	78.43 (69.19–85.96)	48.72 (37.23–60.31)	65.56 (58.12–72.47)	66.67 (61.16–71.75)	63.33 (52.80–72.73)
circFUT8 + CEA + CA19-9	92.16 (85.13–96.55)	29.49 (19.70–40.89)	65.00 (57.55–71.95)	63.09 (59.43–66.60)	74.19 (57.63–85.87)

Values are percentages (95% CIs). Combinations were evaluated using the OR rule, with a combination classified as positive if any constituent marker was positive. **Abbreviations**: ACCU, accuracy; CA19-9, carbohydrate antigen 19-9; CEA, carcinoembryonic antigen; CI, confidence interval; circFUT8, circular RNA derived from FUT8; GC, gastric cancer; NPV, negative predictive value; PPV, positive predictive value; SEN, sensitivity; SPE, specificity.

EARLY

Table 3. Associations between serum circFUT8 expression and clinicopathological characteristics

Parameter	No. of patients	CircFUT8 (high)	CircFUT8 (low)	Unadjusted *p* value	Holm-adjusted *p* value
Gender					
Male	63	34	29	0.308	0.704
Female	39	17	22		
Age, y					
<60	37	18	19	0.837	0.837
≥60	65	33	32		
Tumor size, cm					
<5	70	31	39	0.088	0.369
≥5	32	20	12		
Differentiation grade					
Well or moderately differentiated	55	20	35	0.003	**0.023***
Poorly differentiated or undifferentiated	47	31	16		
T stage					
T1 and T2	55	23	32	0.074	0.369
T3 and T4	47	28	19		
Lymph node status					
Positive	48	30	18	0.017	0.121
Negative	54	21	33		
TNM stage					
I and II	44	17	27	0.046	0.274
III and IV	58	34	24		
Nerve/vascular invasion					
Positive	50	28	22	0.235	0.704

Negative	52	23	29		

Associations were analyzed using Pearson's chi-square test. High and low expression were defined by the median serum circFUT8 level of the 102 patients with GC. Boldface and asterisks indicate statistical significance after Holm correction. *$p < 0.05$. **Abbreviations**: circFUT8, circular RNA derived from FUT8; GC, gastric cancer; TNM, tumor-node-metastasis.

EARLY ACCESS

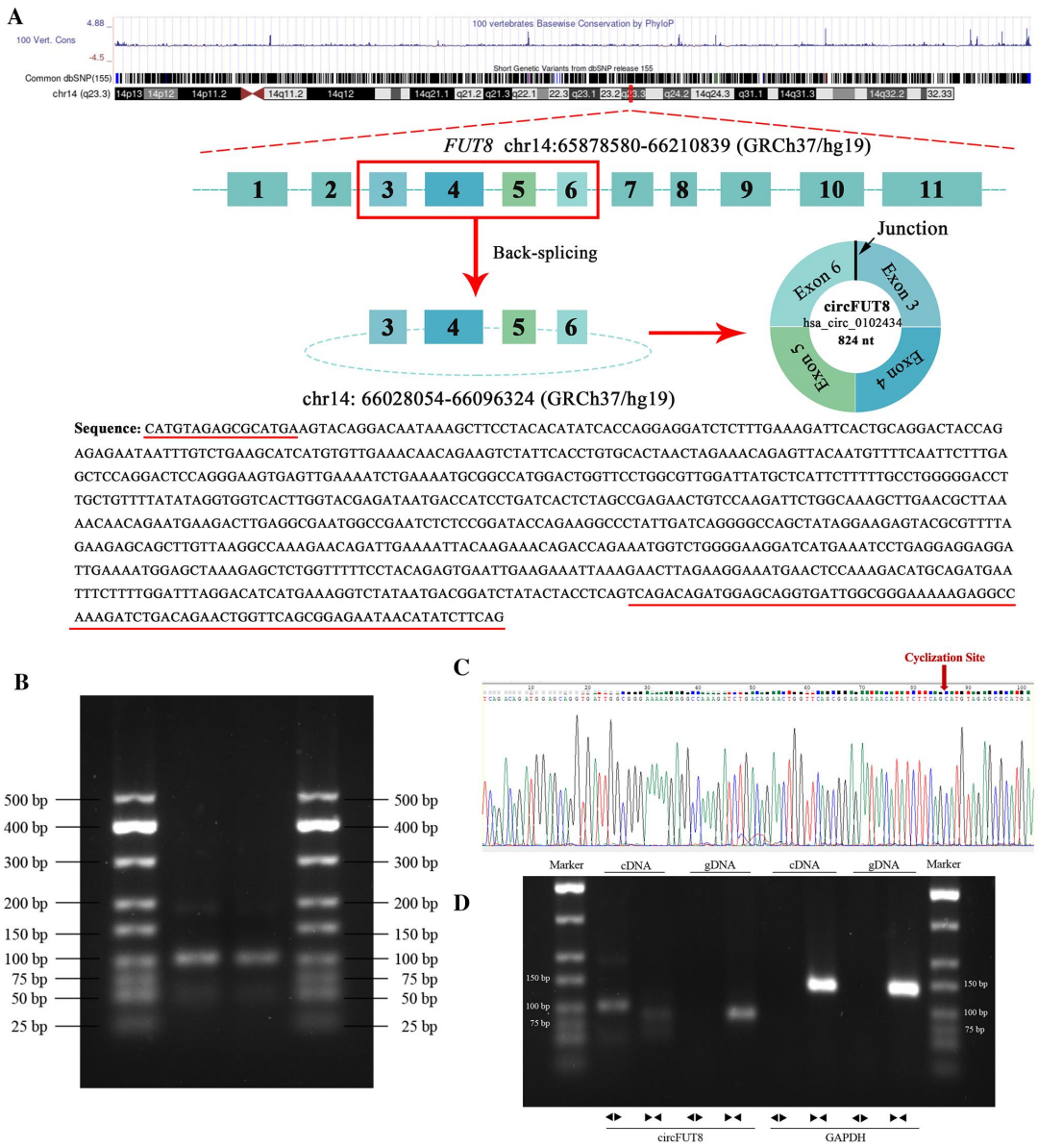


Figure 1. Genomic characteristics and validation of the circular structure of circFUT8. (A) Schematic representation of the genomic location and biogenesis of circFUT8. CircFUT8 (hsa_circ_0102434) is generated by back-splicing of exons 3-6 of the FUT8 gene and is 824 nt in length. Genomic coordinates are based on GRCh37/hg19 and use a 0-based, half-open coordinate system. The sequence and back-splice junction are shown below. **(B)** Agarose gel electrophoresis (AGE) of the PCR product spanning the circFUT8 back-splice junction. The observed product size was consistent with the expected size. **(C)** Sanger sequencing chromatogram of the circFUT8 PCR product. The red arrow indicates the back-splice junction. **(D)** PCR amplification from complementary DNA (cDNA) and genomic DNA (gDNA) using convergent and divergent primers. The divergent primers amplified the expected circFUT8 product from cDNA but not from gDNA. GAPDH served as a linear control.

Abbreviations: AGE, agarose gel electrophoresis; bp, base pairs; cDNA, complementary DNA; chr, chromosome; circFUT8, circular RNA derived from FUT8; dbSNP, Single Nucleotide Polymorphism Database; FUT8, fucosyltransferase 8; GAPDH, glyceraldehyde-3-phosphate dehydrogenase; gDNA, genomic DNA; GRCh37/hg19, Genome Reference Consortium human genome build 37/UCSC hg19; nt, nucleotides; PCR, polymerase chain reaction.

EARLY ACCESS

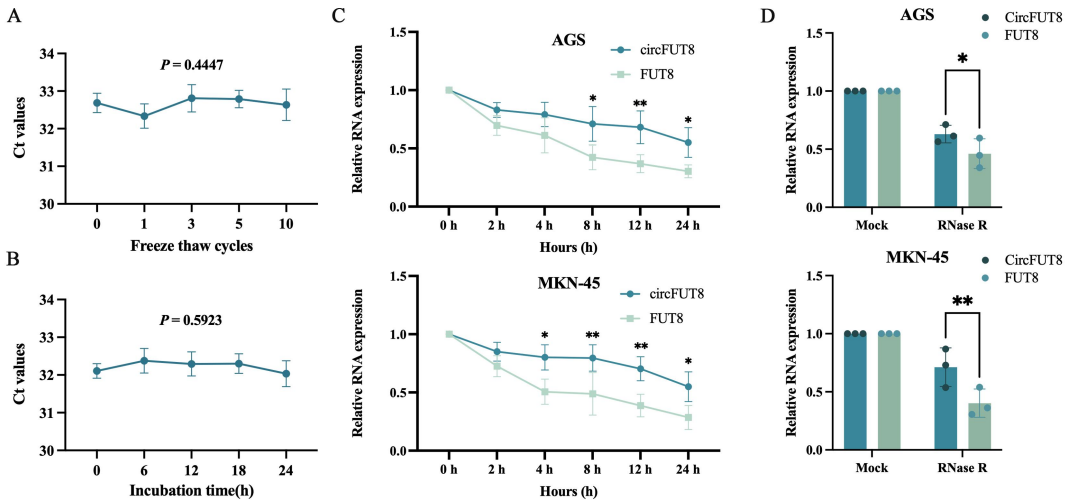


Figure 2. Stability of circFUT8 under preanalytical and experimental conditions. **(A)** Changes in serum circFUT8 Ct values after different numbers of freeze-thaw cycles. No significant difference was observed across 0-10 cycles. **(B)** Changes in serum circFUT8 Ct values after incubation at room temperature for different durations. No significant difference was observed across 0-24 h. **(C)** Relative levels of circFUT8 and its cognate linear FUT8 mRNA in AGS and MKN-45 cells at different time points after actinomycin D treatment. For each RNA species, the expression level at 0 h was normalized to 1. CircFUT8 levels declined more slowly than linear FUT8 mRNA levels, indicating greater stability. **(D)** Relative levels of circFUT8 and linear FUT8 mRNA in AGS and MKN-45 cells following RNase R digestion. For each RNA species, the corresponding mock-treated group was normalized to 1. The proportion of circFUT8 remaining after RNase R digestion was greater than that of linear FUT8 mRNA, indicating greater resistance to RNase R digestion. Mock, samples processed without RNase R. Experiments were independently repeated three times. Data are presented as mean ± SD. *$p < 0.05$; **$p < 0.01$. **Abbreviations**: circFUT8, circular RNA derived from FUT8; Ct, cycle threshold; FUT8, fucosyltransferase 8; mRNA, messenger RNA; RNase R, ribonuclease R; SD, standard deviation.

EARLY ACCESS

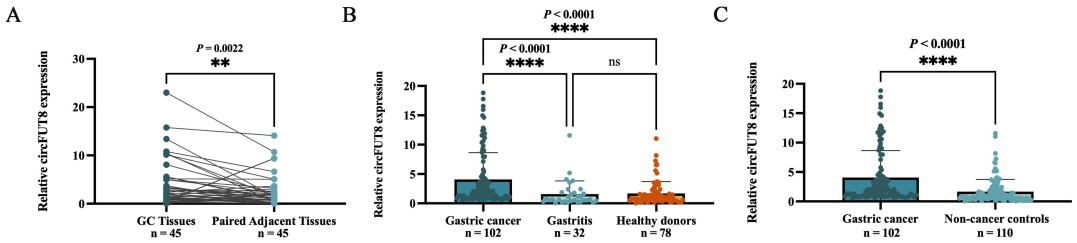


Figure 3. CircFUT8 expression in GC tissues and serum. (A) Relative circFUT8 expression measured by RT-qPCR in 45 paired GC and matched adjacent non-tumor tissue samples. CircFUT8 expression was significantly higher in GC tissues than in matched adjacent non-tumor tissues ($p = 0.0022$). Lines connect paired samples from the same patient. **(B)** Comparison of serum circFUT8 levels among patients with GC ($n = 102$), patients with gastritis ($n = 32$), and healthy controls ($n = 78$). Serum circFUT8 levels were significantly higher in patients with GC than in both control groups (both $p < 0.0001$), whereas no significant difference was observed between patients with gastritis and healthy controls. **(C)** Comparison of serum circFUT8 levels between patients with GC ($n = 102$) and the pooled non-GC control group ($n = 110$), comprising patients with gastritis and healthy controls. Serum circFUT8 levels were significantly higher in patients with GC than in the pooled control group ($p < 0.0001$). Data are presented as mean ± SD. $^{**}p < 0.01$; $^{****}p < 0.0001$. **Abbreviations**: circFUT8, circular RNA derived from FUT8; GC, gastric cancer; ns, not significant; RT-qPCR, real-time quantitative PCR; SD, standard deviation.

EARLY ACCESS

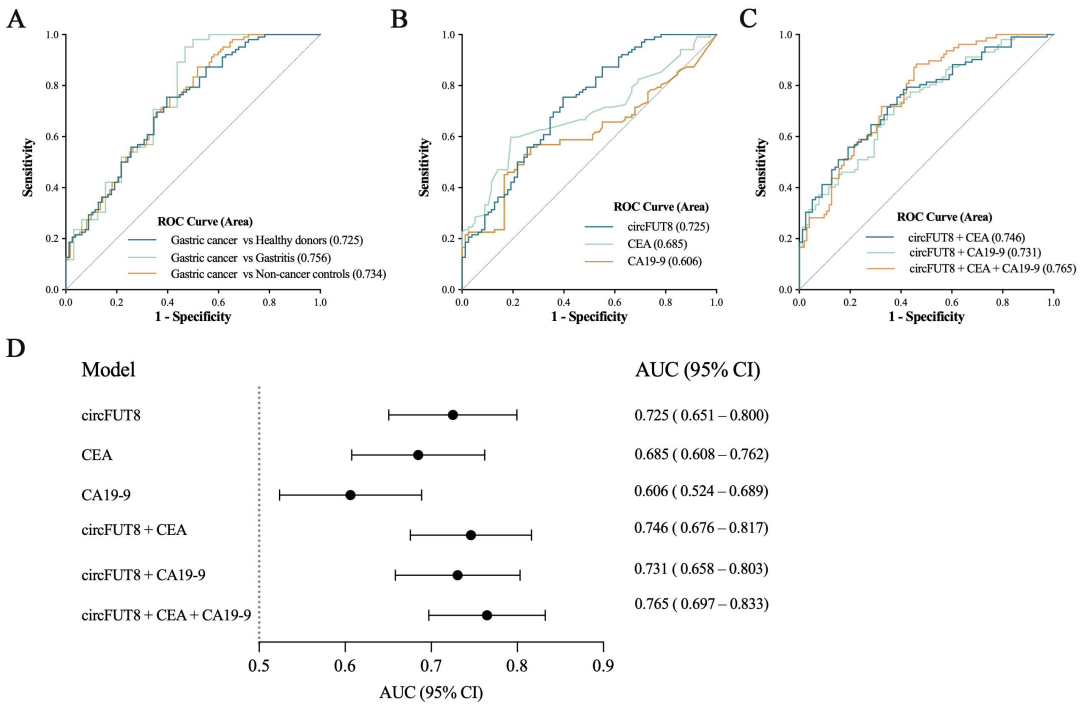


Figure 4. Diagnostic performance of serum circFUT8 for gastric cancer. (A) ROC curves for serum circFUT8 in distinguishing patients with GC from different control groups. The AUCs for distinguishing patients with GC from healthy controls, gastritis, and the pooled non-GC control group were 0.725, 0.756, and 0.734, respectively. The non-GC control group comprised healthy controls and patients with gastritis. **(B)** Comparison of the diagnostic performance of serum circFUT8, CEA, and CA19-9 alone in distinguishing patients with GC from healthy controls. The corresponding AUCs were 0.725, 0.685, and 0.606, respectively. **(C)** ROC curves for circFUT8 in combination with CEA and/or CA19-9 in distinguishing patients with GC from healthy controls. The AUCs for circFUT8 plus CEA, circFUT8 plus CA19-9, and the three-marker panel were 0.746, 0.731, and 0.765, respectively. **(D)** Summary of the AUCs and 95% CIs for circFUT8, CEA, and CA19-9 alone and in combination. Dots represent the AUCs, horizontal lines represent the 95% CIs, and the vertical dashed line at an AUC of 0.5 represents the no-discrimination reference. The AUCs shown are apparent values. **Abbreviations**: AUC, area under the receiver operating characteristic curve; CA19-9, carbohydrate antigen 19-9; CEA, carcinoembryonic antigen; CI, confidence interval; circFUT8, circular RNA derived from FUT8; GC, gastric cancer; ROC, receiver operating characteristic.

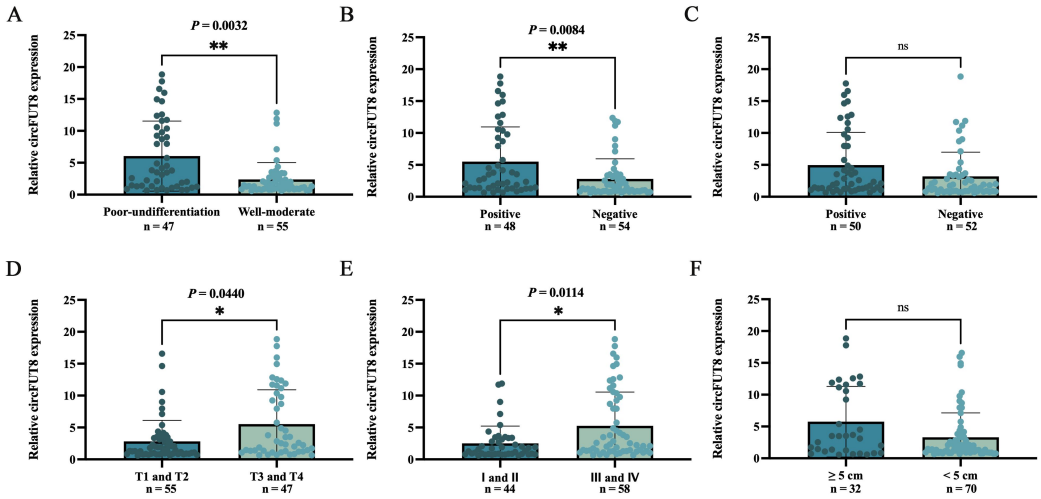


Figure 5. Associations between serum circFUT8 levels and clinicopathological characteristics in GC. (A) Comparison of serum circFUT8 levels according to tumor differentiation. Serum circFUT8 levels were significantly higher in the poorly differentiated or undifferentiated group (n = 47) than in the well or moderately differentiated group (n = 55; p = 0.0032). **(B)** Comparison of serum circFUT8 levels according to lymph node status. Serum circFUT8 levels were significantly higher in patients with lymph node metastasis (n = 48) than in those without lymph node metastasis (n = 54; p = 0.0084). **(C)** Comparison of serum circFUT8 levels according to perineural and/or vascular invasion. No significant difference was observed between the invasion-positive group (n = 50) and the invasion-negative group (n = 52; p = 0.1492). **(D)** Comparison of serum circFUT8 levels according to T category. Serum circFUT8 levels were significantly higher in the T3–T4 group (n = 47) than in the T1–T2 group (n = 55; p = 0.0440). **(E)** Comparison of serum circFUT8 levels according to TNM stage. Serum circFUT8 levels were significantly higher in the stage III–IV group (n = 58) than in the stage I–II group (n = 44; p = 0.0114). **(F)** Comparison of serum circFUT8 levels according to tumor size. No significant difference was observed between patients with a maximum tumor diameter ≥5 cm (n = 32) and those with a maximum tumor diameter <5 cm (n = 70; p = 0.2853). Groups were compared using the Mann-Whitney U test, with Holm correction across eight comparisons, including age and sex comparisons reported in Table S1. All reported p values are Holm-adjusted. Data are presented as mean ± SD. *p < 0.05; **p < 0.01. **Abbreviations**: circFUT8, circular RNA derived from FUT8; GC, gastric cancer; ns, not significant; SD, standard deviation; TNM, tumor-node-metastasis.

EARLY ACCESS

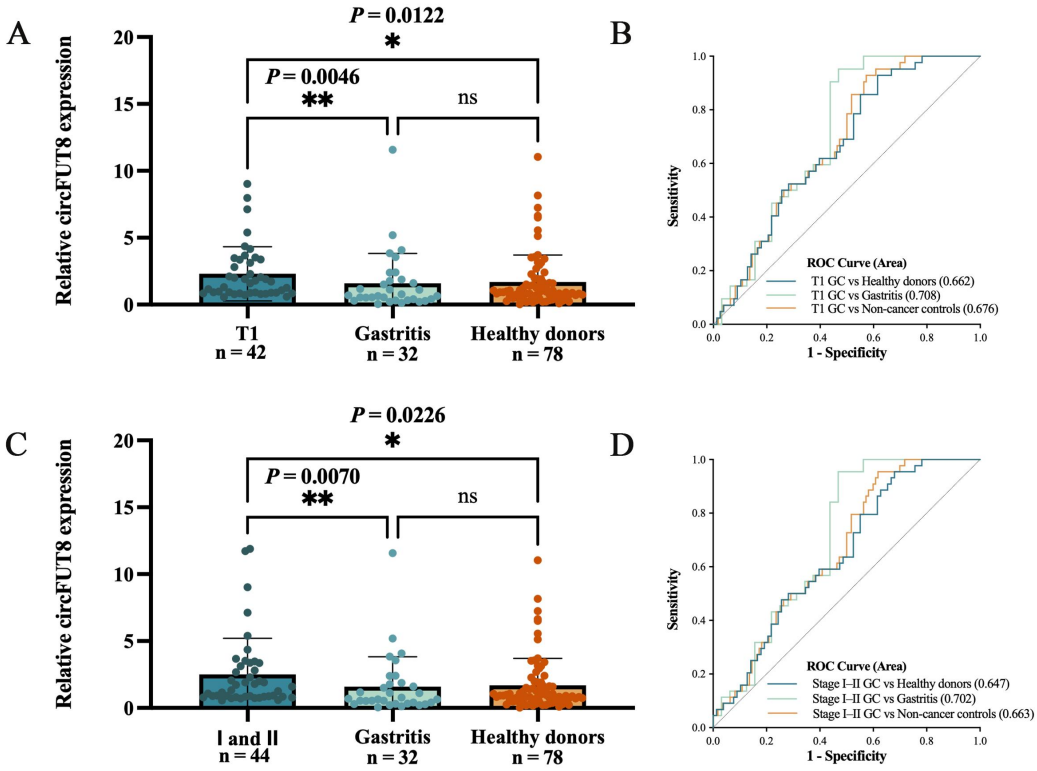


Figure 6. Exploratory diagnostic performance of serum circFUT8 for T1 GC and TNM stage I–II GC. (A) Serum circFUT8 levels in patients with T1 GC (n = 42), patients with gastritis (n = 32), and healthy controls (n = 78). Levels were higher in T1 GC than in gastritis (p = 0.0046) and healthy controls (p = 0.0122). **(B)** ROC curves for T1 GC versus healthy controls, gastritis, and pooled non-GC controls; the respective AUCs were 0.662, 0.708, and 0.676. **(C)** Serum circFUT8 levels in TNM stage I–II GC (n = 44) versus the same control groups. Levels were higher in stage I–II GC than in gastritis (p = 0.0070) and healthy controls (p = 0.0226). Neither **(A)** nor **(C)** showed a significant difference between control groups. **(D)** ROC curves for stage I–II GC versus healthy controls, gastritis, and pooled non-GC controls; the respective AUCs were 0.647, 0.702, and 0.663. Pooled controls comprised patients with gastritis and healthy controls. Table S2 provides 95% CIs. Data are mean ± SD. *$p < 0.05$; **$p < 0.01$. **Abbreviations**: AUC, area under the receiver operating characteristic curve; CI, confidence interval; circFUT8, circular RNA derived from FUT8; GC, gastric cancer; ns, not significant; ROC, receiver operating characteristic; SD, standard deviation; TNM, tumor-node-metastasis.

SUPPLEMENTAL DATA

Table S1. Associations between continuous serum circFUT8 levels and clinicopathological characteristics before and after Holm correction

Parameter	Unadjusted *p* value	Holm-adjusted *p* value
Gender	0.3130	0.6260
Age	0.9008	0.9008
Tumor size	0.0951	0.2853
Differentiation grade	0.0004	**0.0032****
T stage	0.0088	**0.0440***
Lymph node status	0.0012	**0.0084****
TNM stage	0.0019	**0.0114***
Nerve/vascular invasion	0.0373	0.1492

Serum circFUT8 expression was analyzed as a continuous variable. Boldface and asterisks indicate statistical significance after Holm correction. *$p < 0.05$; **$p < 0.01$.

Abbreviations: circFUT8, circular RNA derived from FUT8; TNM, tumor-node-metastasis.

EARLY ACCESS

Table S2. Exploratory diagnostic performance of serum circFUT8 for T1 and TNM stage I–II GC

GC subgroup (*n*)	Control group (*n*)	AUC (95% CI)
T1 (42)	Healthy controls (78)	0.662 (0.566–0.759)
T1 (42)	Gastritis (32)	0.708 (0.577–0.838)
T1 (42)	Pooled non-GC controls (110)	0.676 (0.590–0.761)
TNM stage I–II (44)	Healthy controls (78)	0.647 (0.549–0.744)
TNM stage I–II (44)	Gastritis (32)	0.702 (0.572–0.832)
TNM stage I–II (44)	Pooled non-GC controls (110)	0.663 (0.576–0.750)

Pooled non-GC controls comprised healthy controls and patients with gastritis. **Abbreviations**: AUC, area under the receiver operating characteristic curve; CI, confidence interval; circFUT8, circular RNA derived from FUT8; GC, gastric cancer; TNM, tumor-node-metastasis.

EARLY ACCESS